Influence of matrix metalloproteinase MMP-9 on dendritic spine morphology

Michaluk, Piotr; Wawrzyniak, Marcin; Alot, Przemyslaw; Szczot, Marcin; Wyrembek, Paulina; Mercik, Katarzyna; Medvedev, Nikolay; Wilczek, Ewa; De Roo, Mathias; Zuschratter, Werner; Muller, Dominique; Wilczynski, Grzegorz M; Mozrzymas, Jerzy W; Stewart, Michael G [**and 2 more**]

Influence of matrix metalloproteinase MMP-9 on dendritic spine morphology

Piotr Michaluk[1,2,*], Marcin Wawrzyniak[1], Przemyslaw Alot[1], Marcin Szczot[3], Paulina Wyrembek[3], Katarzyna Mercik[3], Nikolay Medvedev[4], Ewa Wilczek[5], Mathias De Roo[6], Werner Zuschratter[7], Dominique Muller[6], Grzegorz M. Wilczynski[5], Jerzy W. Mozrzymas[3], Michael G. Stewart[4], Leszek Kaczmarek[1,*] and Jakub Wlodarczyk[1,*]

[1]Department of Molecular and Cellular Neurobiology, The Nencki Institute, Pasteura 3, 02-093 Warsaw, Poland
[2]Department of Physiological Chemistry and Centre for Biomedical Genetics, University Medical Center Utrecht, Universiteitsweg 100, 3584 CG Utrecht, The Netherlands
[3]Laboratory of Neuroscience, Department of Biophysics, Wroclaw Medical University, Chalubinskiego 3, 50-367 Wroclaw, Poland
[4]Department of Life Sciences, The Open University, Milton Keynes MK7 6AA, UK
[5]Department of Neurophysiology, The Nencki Institute, Pasteura 3, 02-093 Warsaw, Poland
[6]Department of Neuroscience, Faculty of Medicine, University of Geneva, 1 rue Michel-Servet, CH-1211 Geneva 4, Switzerland
[7]Laboratory for Electron- and Laserscanning Microscopy, Leibniz Institute for Neurobiology, Brenneckestraße 6, 39118 Magdeburg, Germany
*Authors for correspondence (p.michaluk@nencki.gov.pl; l.kaczmarek@nencki.gov.pl; j.wlodarczyk@nencki.gov.pl)

Summary

An increasing body of data has shown that matrix metalloproteinase-9 (MMP-9), an extracellularly acting, Zn^{2+}-dependent endopeptidase, is important not only for pathologies of the central nervous system but also for neuronal plasticity. Here, we use three independent experimental models to show that enzymatic activity of MMP-9 causes elongation and thinning of dendritic spines in the hippocampal neurons. These models are: a recently developed transgenic rat overexpressing autoactivating MMP-9, dissociated neuronal cultures, and organotypic neuronal cultures treated with recombinant autoactivating MMP-9. This dendritic effect is mediated by integrin β1 signalling. MMP-9 treatment also produces a change in the decay time of miniature synaptic currents; however, it does not change the abundance and localization of synaptic markers in dendritic protrusions. Our results, considered together with several recent studies, strongly imply that MMP-9 is functionally involved in synaptic remodelling.

Key words: Brain, Extracellular matrix, Plasticity, Proteases, MMP-9

Introduction

It has been clearly established that experience modifies functional circuits in the brain (Chklovskii et al., 2004). Furthermore, it has been shown that changes in the morphology of dendritic spines, carrying postsynaptic domains of excitatory synapses, might be involved in synaptic plasticity, as well as in learning and memory (Holtmaat and Svoboda, 2009; Holtmaat et al., 2006; Moser et al., 1994; Xu et al., 2009). Moreover, induction of long-term potentiation (LTP) is associated with spine growth (De Roo et al., 2008b; Matsuzaki et al., 2004; Yang et al., 2008), whereas induction of long-term depression (LTD) is associated with spine shrinkage (Zhou et al., 2004).

Recent studies have indicated that spine structure can be regulated by extracellular matrix (ECM) proteins, such as reelin (Niu et al., 2008), as well as cell surface proteins [e.g. N-cadherin (Mysore et al., 2007), ephrin receptors (Moeller et al., 2006) and integrins (Shi and Ethell, 2006)]. Whereas the exact mechanism of this regulation is poorly understood, extracellularly acting proteases targeting ECM and/or surface proteins have recently been implicated in different forms of neuronal plasticity (Brown et al., 2009; Dityatev et al., 2010; Mizoguchi et al., 2007; Pizzorusso et al., 2002; Rivera et al., 2010).

Matrix metalloproteinases (MMPs) are predominantly secreted extracellular endopeptidases that can modify ECM components

and control cell behavior (Mott and Werb, 2004; Sternlicht and Werb, 2001). Their expression and activity are tightly regulated; they are expressed (often in response to a cell activation) in an inactive form and require enzymatic processing in order to reveal the catalytic site. Once activated, they can be inhibited by tissue inhibitors of metalloproteinases (TIMPs) but their activity is also regulated by glycosylation and internalization (Yong, 2005). Previously MMP-9 was believed to be associated mainly with pathologies of the brain, such as ischemia, gliomas or epilepsy (Asahi et al., 2000; Gu et al., 2002; Wilczynski et al., 2008; Yong, 2005); however, recently its involvement in brain physiology has been partially elucidated (Nagy et al., 2006; Szklarczyk et al., 2002).

An involvement of MMPs in modulation of morphology of dendritic spines has recently been observed. Bilousova et al. (Bilousova et al., 2006) showed that MMP-7, in an N-methyl-D-aspartate (NMDA)-dependent manner, appears to cause transformation of mature mushroom-shaped spines into long filopodia-like structures in cultures of dissociated neuronal cells. Tian et al. (Tian et al., 2007), also in dissociated cultures, showed that either MMP-2 or MMP-9, through cleavage of the intercellular adhesion molecule-5 (ICAM-5), can also cause elongation of dendritic filopodia. Furthermore, Wang et al. (Wang et al., 2008) showed that in acute hippocampal slices MMP-9 was

necessary for the enlargement of spines associated with LTP induction. Notably, Bilousova et al. (Bilousova et al., 2009) showed that in the fragile X mouse model (*Fmr1*-knockout mice) there was an increase in the ratio of filopodia to mature spines; this effect could be reversed by minocycline, whose pleiotropic effects include the ability to inhibit MMP-9 expression. Furthermore, an incubation of a dissociated neuronal cell culture with recombinant MMP-9 caused transformation of dendritic spines from mushroom- into filopodia-like protrusions (Bilousova et al., 2009).

Here, we set out to verify directly the effects of MMP-9 on spine morphology. Recombinant autoactivating MMP-9 (Fisher et al., 2002) was either introduced into the rat brain in the form of a neuronally overexpressed transgene, or produced in a heterologous baculoviral expression system as a recombinant protein. Because MMP-9 has been shown to exert some effects independently of its enzymatic activity (e.g. through specific protein–protein interactions) (Ezhilarasan et al., 2009; Redondo-Munoz et al., 2010), we also produced a non-enzymatically-active form of the MMP-9 and tested its effects on spine morphology.

Results

Transgenic rats overexpressing an autoactivating mutant of MMP-9 display longer and thinner dendritic spines

In order to observe the influence of enzymatic activity of MMP-9 on dendritic spines in vivo, we compared spine shapes in transgenic rats overexpressing autoactivating mutants of MMP-9 under the control of the synapsin I promoter (MMP-9 transgenic rats; MMP-9 TR) with spines in wild-type (WT) rats (Wilczynski et al., 2008). Morphometric analysis of spines in neurons stained with a lipophilic dye, DiI was carried out in the CA1 area of the hippocampus (Fig. 1A). In our studies, we used a scale-free parameter, the length-to-width ratio (i.e. the length divided by the width), which reflects the spine shape (see Discussion) and thus

effectively describes the spine form. MMP-9 TR rats displayed an larger average length-to-width ratio (2.845 ± 0.119, $n=4$ rats) than did WT rats (2.057 ± 0.112, $n=4$ rats) (Student's t-test revealed that there was a significant difference in the spine shape parameter, length:width, of MMP-9 TR compared with WT rats; $t=3.914$, $P=0.0021$; Fig. 1B). Interestingly, the spine density in MMP-9 TR was unchanged in comparison with WT rats (Student's t-test did not show a significant difference; $t=0.4178$, $P=0.6907$; Fig. 1C). We did not observe differences in spine length between WT rats (1.782 ± 0.0434 μm) and MMP-9 TR (1.826 ± 0.0258 μm) ($t=0.8843$, $P=0.4106$); however, there was a significant difference ($t=2.497$, $P=0.0467$) in the width of the spine head between WT rats (0.7292 ± 0.0280 μm) and MMP-9 TR (0.6443 ± 0.0193 μm).

In addition, spine morphology was analysed using transmission electron microscopy and subsequent three-dimensional reconstruction of series of ultrathin sections, and we also performed analyses of synaptic densities and the categories of synapses. There were no differences in synaptic densities between WT rats (294.61 ± 19.883 synapses per 100 μm^3) and MMP-9 TR (323.56 ± 27.53 synapses per 100 μm^3) ($F_{1,8}=0.72632$; $P=0.4421$). To determine whether there were changes in the morphology of mushroom and thin dendritic spines, we reconstructed 75 mushroom and 75 thin spines and their postsynaptic densities (PSDs) from WT and TR rats. Fig. 1D shows examples of these two categories of spines (the left-hand panel of Fig. 1D shows four electron micrographs, and the right-hand panel reconstructions of two mushroom and two thin spines). Fig. 1E shows that there was a statistically significant decrease in the proportion of mushroom spines in CA1 area of MPP-9 TR (10.62 ± 0.92) compared with WT rats (15.1 ± 1.17) ($F_{1,8}=9.0588$; $P=0.0395$) with a corresponding increase in the proportion of thin spines in MPP-9 TR (86.69 ± 1.46) compared with WT rats
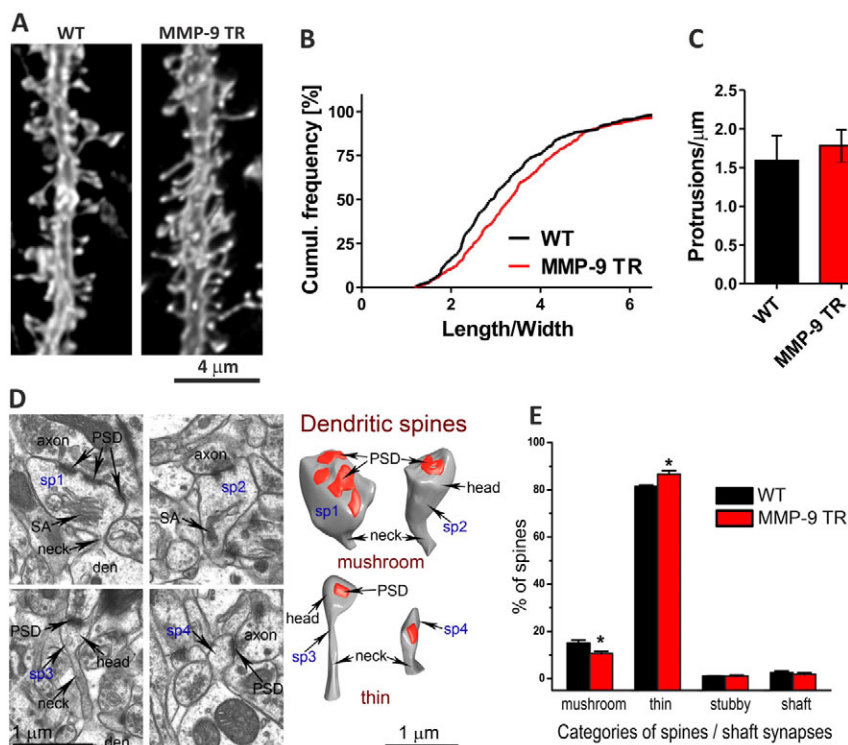
Fig. 1. Transgenic rats overexpressing autoactivating mutant of MMP-9 have longer and thinner dendritic spines. (**A**) Examples of DiI-stained neurons in the CA1 area of rat hippocampus of wild-type (WT) and transgenic rats overexpressing the autoactivating mutant of MMP-9 under the control of the synapsin I promoter (MMP-9 TR). Pictures represent secondary apical dendrites. (**B**) Cumulative frequency of the shape parameter (length/width) of spines in WT and MMP-9 TR rats. Student's t-test revealed a significant difference in the spine shape parameter of WT compared with MMP-9 TR rats ($t=3.914$; $P=0.0021$). (**C**) Mean ($\pm$ s.e.m) spine density in WT and MMP-9 TR rats. Student's t-test did not show significant differences ($t=0.5225$; $P=0.6154$). (**D**) Examples of mushroom and thin spines in the CA1 area: the left-hand panel shows four electron microscopic images of two mushroom (sp1, sp2) and two thin (sp3, sp4) dendritic spines; the right-hand panel shows a three-dimensional reconstruction of these four spines. PSD, post-synaptic density; head, spine head; neck, spine neck; den, dendrite; axon, presynaptic varicosity; SA, spine apparatus. (**E**) Redistribution of dendritic spines between the four main categories of spines and synapses (mean $\pm$ s.e.m.). One-way ANOVA showed that there is a significant decrease in the proportion of mushroom spines in MPP-9 TR compared with WT ($F=9.0588$, $P=0.0395$), whereas the proportion of thin spines increases ($F=11.2548$; $P=0.0284$).

(81.39 ± 0.66) $(F_{1,8}=11.2549; P=0.02844)$. However, no changes were found in the proportion of stubby spines and shaft synapses (Fig. 1E). No changes were found in the size of mushroom and thin spines and their PSDs in MPP-9 TR compared with WT rats. To describe possible changes in spine shape in the active zone area, we analysed the curvature of the PSD area of mushroom and thin spines [as described in the Materials and Methods and in Popov et al. (Popov et al., 2008)] but no significant changes were found in spine curvature. The curvature of mushroom spines in the PSD area was $(-4.66 \pm 1.40°$ for WT rats and $-0.19 \pm 1.33°$ for MMP-9 TR $(F_{1,8}=0.6148; P=0.4768)$; the curvature of thin spines in the PSD area was, respectively, $-6.25 \pm 0.53°$ for WT and $-1.34 \pm 0.62°$ for MMP-9 TR rats $(F_{1,8}=1.1313; P=0.3474)$.

Production of autoactivating MMP-9 and its non-active analogue

In order to examine the influence of MMP-9 on the morphology of dendritic spines, we applied a recombinant autoactivating mutant of MMP-9 (Fisher et al., 2002). For protein expression we used the Bac-to-Bac baculovirus expression system. Recombinant baculovirus was used for infection of High-Five cells and conditioned medium was collected for analysis of expression by gel zymography. At 24, 48 and 72 hours after infection, medium was collected and equal volumes were subjected to gel zymography. The largest expression level was observed at 48 hours post infection (Fig. 2A). We then used the cell medium at 48 hours after infection with baculovirus for purification of the recombinant autoactivating mutant of MMP-9, using affinity chromatography on gelatine–Sepharose resin. The left-hand panel of Fig. 2B shows an SDS-PAGE gel of the recombinant MMP-9 after purification, and the protein identity was confirmed by western blotting and gel zymography (Fig. 2B middle and right-hand panel respectively). In order to obtain the non-enzymatically active form of MMP-9, glutamate 402 in the catalytic centre of the autoactivating mutant was replaced by alanine, so that enzyme activity was lost. To produce the recombinant inactive mutant (E402A) of autoactivating MMP-9

we again used the Bac-to-Bac baculovirus expression system. The expression and purification procedure was the same as for autoactivating MMP-9. We obtained protein with the same molecular mass as autoactivating MMP-9 and with the same immunoreactivity with anti-human-MMP-9 antibody, but without enzymatic activity, as determined by gel zymography (Fig. 2B). We then checked the enzymatic activity of the obtained recombinant MMP-9 and MMP-9 E402A in solution using DQ-gelatine, a standard fluorescence substrate for gelatinases. As expected, MMP-9 displayed strong enzymatic activity in solution, whereas MMP-9 E402A did not (Fig. 2C). We also tested the potency of commercially available inhibitors of MMPs towards recombinant MMP-9 at standard concentration employed in our experiments (i.e. 400 ng/ml). Indeed the broad-spectrum MMP inhibitor GM6001 and the more specific Inhibitor-I were able to effectively decrease the activity of MMP-9. Importantly, 0.1% DMSO, which was a solvent for both inhibitors, in solution affected MMP-9 activity only slightly (Fig. 2C).
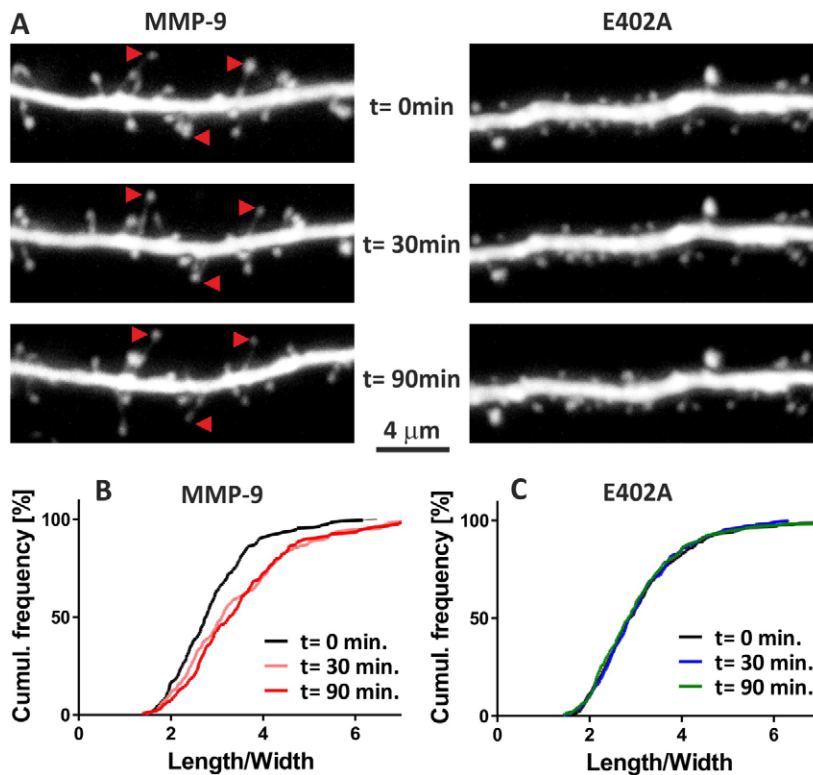
Live imaging of neurons in organotypic hippocampal cultures reveals the influence of active MMP-9 on dendritic spines

To observe the influence of MMP-9 on spines in a simpler model than live animals, and one which allows easier manipulation and temporal observations, we employed an organotypic hippocampal culture and live imaging of the dendrites. After transfection with a pcDNA3-eGFP plasmid using a biolistic method, hippocampal pyramidal neurons of CA1 area, which expressed eGFP, were visualized in a confocal microscope. Slices were treated with either recombinant MMP-9 or MMP-9 E402A, and images were taken following 30 and 90 minutes of incubation (Fig. 3A–C). The length-to-width parameter was used to evaluate the spine shape and a one-way ANOVA showed a significant difference between groups in cultures incubated with the MMP-9 $(F=8.206, P=0.0023; n=8$ cells) and post-hoc Tukey test reached significance for $t=0$ (2.930 ± 0.100) compared with the MMP-9 incubation for 30 minutes (3.433 ± 0.1564) $(P=0.05)$ and for
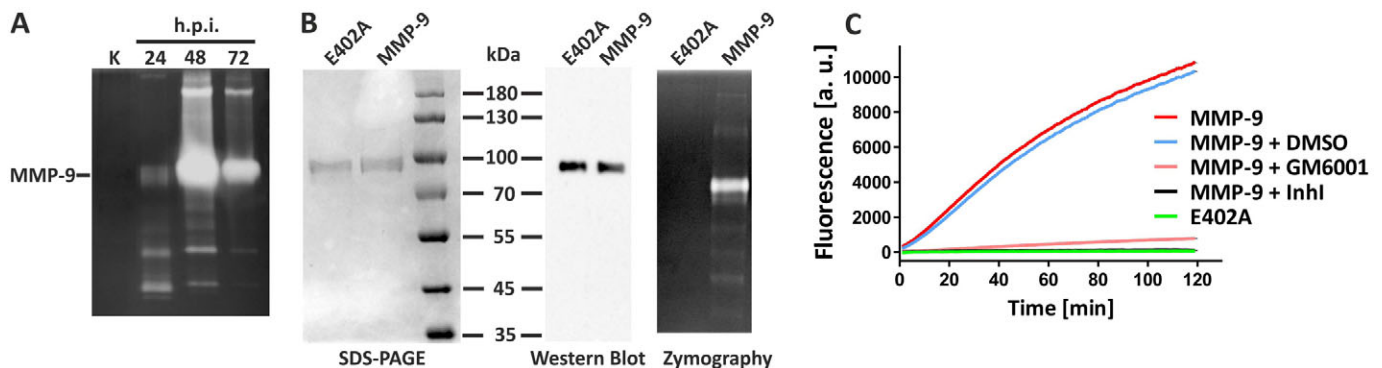
Fig. 2. **Expression and analysis of purified recombinant autoactivating mutant of MMP-9 and its inactive mutant MMP-9 E402A.** (**A**) Gel zymography of samples of culture medium from High-Five cells infected with recombinant baculovirus carrying autoactivating MMP-9. The biggest activity, and thus protein concentration, is observed 48 hours post infection (h.p.i.). (**B**) Left-hand panel: SDS-PAGE gel of purified MMP-9 and MMP-9 E402A confirms the molecular mass of the purified protein; middle panel: western blot for human MMP-9 confirms that the purified protein is human MMP-9; right-hand panel: gel zymography shows the enzymatic activity of MMP-9 and the lack of this activity in the mutated protein MMP-9 E402A. (**C**) Enzymatic assay using DQ-gelatine (a fluorescent substrate of gelatinases, including MMP-2 and -9). 400 ng/ml of purified protein was incubated with DQ-gelatine in 37℃ and fluorescence was measured every minute. MMP-9 activity (red line) can be inhibited by the general MMP inhibitor GM6001 (25 µM; pink line) or the more specific Inhibitor I of MMP-9 and -13 (5 µM; black line). The inactive mutant MMP-9 E402A does not show enzymatic activity in this assay (green line). 0.1% DMSO, the diluent of the inhibitors slightly decreases the activity of autoactivating MMP-9 (blue line).

Fig. 3. Live imaging of organotypic hippocampal culture reveals the influence of the enzymatic activity of MMP-9 on spine morphology. (A) A fragment of secondary apical dendrite from a pyramidal neuron expressing eGFP was visualized with a confocal microscope ($t=0$) and then treated with recombinant MMP-9 or MMP-9 E402A at a final concentration of 400 ng/ml. The dendrite was imaged again after 30 and 90 minutes of incubation (middle and lower panels respectively). Red arrowheads show examples of spines changing shape after incubation with MMP-9. (B) Cumulative frequency of the shape parameter (length/width) of spines in the group incubated with MMP-9. One-way ANOVA showed that there is a significant difference in the shape parameter between groups of cultures incubated with MMP-9 ($F=8.206$, $P=0.0023$) and post-hoc Tukey's test reached significance for $t=0$ compared with MMP-9 after 30 minutes ($P=0.05$) and for $t=0$ compared with MMP-9 at 90 minutes ($P=0.001$). (C) The cumulative frequency of the shape parameter (length/width) of spines in the group incubated with MMP-9 E402A. One-way ANOVA did not reach significance ($F=0.04136$; $P=0.9595$).

90 minutes (3.713 ± 0.152) ($P=0.001$). We observed no changes in the shape parameter (length:width, L:W) in cultures treated with inactive protease MMP-9 E402A (one-way ANOVA failed to reach significance; $F=0.04065$, $P=0.9602$; $n=9$ cells), which was found to be: L:W$_{t=0}$, 3.214 ± 0.196; L:W$_{t=30}$, 3.197 ± 0.124 and L:W$_{t=90}$, 3.264 ± 0.188.

The enzymatic activity of MMP-9 causes changes in dendritic spine morphology producing longer and thinner spines in dissociated cultures

To investigate further the influence of MMP-9 on morphology of dendritic spines, and to extend the results obtained with the aforementioned models, we used dissociated hippocampal cultures. Neurons were transfected with plasmid vector carrying eGFP under the control of the β-actin promoter and after 15 days in vitro the cells were incubated with recombinant autoactivating form of MMP-9 for either 30 or 90 minutes. As a control, we used hippocampal cultures incubated with either the non-active mutant of MMP-9 or a buffer devoid of recombinant proteins. After fixing the cultures, we utilized immunofluorescence labelling of neurons expressing eGFP and analysed the density and morphology of protrusions (Fig. 4B–E). Notably, MMP-9 treatment did not affect the overall morphology of the cultures and there was no visible change in neurites (Fig. 4A). Moreover, incubation with MMP-9 did not affect the total density (mean density in buffer after 90 minutes, 1.058 ± 0.106 μm^{-1}; mean density with MMP-9 E402A after 90 minutes, 1.025 ± 0.101 μm^{-1}; mean density with MMP-9 after 30 minutes, 1.103 ± 0.04120 μm^{-1}; mean density MMP-9 after 90 minutes, 0.9819 ± 0.06754 μm^{-1}; $F=0.3787$, $P=0.7694$, $n=6$ cells) of dendritic protrusions (Fig. 4C). However, a one-way ANOVA of the shape parameter revealed differences between groups ($F=15.61$, $P<0.0001$, $n=6$ cells) and a post-hoc Tukey test showed that by 30 minutes of incubation with

MMP-9 there were significant increases in the length:width parameter, which by 90 minutes of incubation were increased further (L:W with buffer for 90 minutes, 1.883 ± 0.05692; L:W with MMP-9 for 30 minutes, 2.509 ± 0.1255; L:W with MMP-9 for 90 minutes, 2.940 ± 0.2199) (Fig. 4D). This effect can be visualized more easily by a cumulative frequency distribution of analysed spines in each group (Fig. 4E). Furthermore, we were interested to determine whether the enzymatic activity of MMP-9 is necessary to induce changes in morphology of spines. Hence, we incubated cultures for 90 minutes with the inactive mutant MMP-9 E402A; this did not influence either the shape of dendritic protrusions or their overall density (L:W MMP-9 E402A, 1.806 ± 0.1153) (Fig. 4B–E). We did not observed significant changes either in the length of protrusions (length in buffer after 90 minutes, 1.165 ± 0.06998 μm; length with MMP-9 E402A after 90 minutes, 1.301 ± 0.1114 μm; length with MMP-9 after 30 minutes, 1.419 ± 0.1047 μm; length with MMP-9 after 90 minutes, 1.746 ± 0.3431 μm; $F=1.685$, $P=0.2023$, $n=6$ cells) or in the width of spine heads (width in buffer after 90 minutes 0.6208 ± 0.04934 μm; width with MMP-9 E402A after 90 minutes, 0.7742 ± 0.06082 μm; width with MMP-9 after 30 minutes, 0.5818 ± 0.02733 μm; width with MMP-9 after 90 minutes, 0.6580 ± 0.07878 μm; $F=2.110$, $P=0.1310$, $n=6$ cells).

Enzymatic activity of MMP-9 does not change the abundance of the presynaptic marker protein bassoon or its localization in the protrusions

To characterize further the influence of MMP-9 on synaptic morphology and to check whether the longer and thinner protrusions are potentially functional, we analysed the abundance of the presynaptic marker protein bassoon and the postsynaptic marker homer 1, which are often used to distinguish mature spines and synapses (Grabrucker et al., 2009; Konopka et
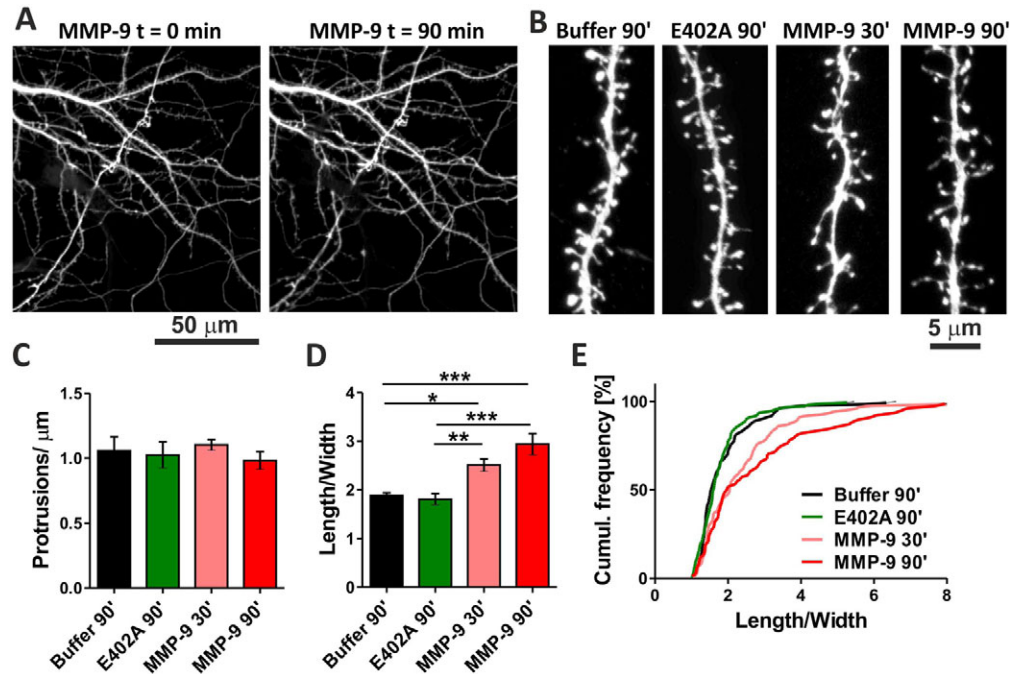
Fig. 4. MMP-9 enzymatic activity makes dendritic spines in dissociated hippocampal culture longer and thinner but does not change the dendritic arbor. (**A**) Live imaging of 15 DIV hippocampal neurons, expressing eGFP, incubated with MMP-9 does not reveal changes in the structure and number of neurites. (**B**) Maximal projections of confocal scans of a dissociated hippocampal culture transfected with a plasmid carrying eGFP under the control of the β-actin promoter. After reaching an age of at least 15 DIV, cells were incubated for 30 and 90 minutes with 400 ng/ml of active MMP-9, or for 90 minutes with inactive MMP-9 E402A or the buffer used for elution of recombinant protein from the affinity column. (**C**). Mean ($\pm$ s.e.m.) protrusion density. One-way ANOVA did not reveal significant differences between groups of mean protrusions density calculated per cell ($F=0.936$; $P=0.4353$). (**D**) Mean ($\pm$ s.e.m.) shape parameter (length/width). One-way ANOVA revealed significant differences between groups of mean shape parameter calculated per cell ($F=15.61$; $P<0.0001$). Post-hoc Tukey's tests reached significance for buffer compared with MMP-9 at 30 minutes (*$P<0.05$) and 90 minutes (***$P<0.001$), for MMP-9 E402A compared with MMP-9 at 30 minutes (**$P<0.01$) and for MMP-9 E402A compared with MMP-9 at 90 minutes (***$P<0.001$). (**E**) The cumulative frequency of the shape parameter (length/width).

al., 2010; Petrini et al., 2009; Verpelli et al., 2010). We incubated dissociated hippocampal cultures at 15 days in vitro (DIV) with buffer, recombinant MMP-9 or MMP-9 E402A for 90 minutes, then fixed the specimens and stained for the synaptic markers using immunofluorescence. One-way ANOVA did not reveal any changes in localization of synaptic markers in dendritic spines between the examined groups, measured as the percentage of bassoon- or homer-1-positive protrusions: bassoon with buffer, $62.67\pm1.138\%$, $n=13$ cells; bassoon with MMP-9 E402A, $66.41\pm1.340\%$, $n=8$ cells, bassoon with MMP-9, $63.19\pm1.564\%$, $n=11$ cells; $F=1.904$, $P=0.1671$ (Fig. 5A–C); homer with buffer, $62.28\pm1.66\%$, $n=13$ cells, homer with MMP-9 E402A, $66.67\pm1.71\%$, $n=8$ cells; homer with MMP-9, $63.61\pm1.60\%$, $n=11$ cells; $F=1.605$, $P=0.2183$ (Fig. 5D–F). We also did not observe any changes in the density of synaptic markers after incubation with recombinant MMP-9, measured as number of clusters per μm of examined dendrite (bassoon with buffer, 1.041 ± 0.0513 μm^{-1}, $n=13$ cells, bassoon with MMP-9 E402A, 1.090 ± 0.0609 μm^{-1}, $n=8$ cells, bassoon with MMP-9, 0.9791 ± 0.09308 μm^{-1}, $n=11$ cells; $F=0.5418$, $P=0.5875$; homer with buffer, 1.028 ± 0.0658 μm^{-1}, $n=13$ cells, homer with MMP-9 E402A, 0.8500 ± 0.0810 μm^{-1}, $n=8$ cells; homer with MMP-9, 0.8091 ± 0.0760 μm^{-1}, $n=11$ cells; $F=2.792$, $P=0.0778$).

The enzymatic activity of MMP-9 affects spine physiology

Because it is known that alterations of spine morphology associated with plasticity phenomena, such as LTP and LTD, are accompanied by profound functional changes at glutamatergic synapses, we wanted to test whether MMP-9 activity, besides affecting spine geometry, also influences the electrophysiological properties of synapses in our model. To this end, we used patch-clamping and recorded glutamatergic miniature excitatory synaptic currents (mEPSCs) in the whole-cell mode ($V_m=-70$ mV) from dissociated hippocampal neurons. Neurons were incubated in the presence of autoactivating MMP-9, MMP-9 E402A or protein buffer for up to 90 minutes and the impact of treatment was checked after 30, 60 and 90 minutes. We found that such treatment did not significantly affect the mean current amplitude of minis (31.38 ± 4.02 pA, $n=6$; 34.08 ± 4.05 pA, $n=7$; 28.53 ± 3.07 pA, $n=7$ for MMP-9, E402A and buffer, respectively; $P>0.05$, unpaired Student's t-test, Fig. 6A,B). However, the functional impact of synaptic currents depends not only on amplitude but also on the timecourse. In particular, synaptic current duration (typically assessed as the weighted decay time constant) can strongly affect synaptic integration and this parameter is known to undergo a developmental increase that is strictly correlated with alterations in synapse geometry (Cathala et al., 2005; Wall et al., 2002). Treatment of neurons with MMP-9, MMP-9 E402A or buffer had no significant effect on the mEPSC decay time course in neurons treated for 30 or 60 minutes (data not shown). However, 90 minutes of treatment with MMP-9, resulted in a significant increase in the decay time constant with respect to buffer- or MMP-9-E402A-treated neurons (5.96 ± 0.91 ms, $n=7$; 3.89 ± 0.53 ms, $n=6$; 3.61 ± 0.51 ms, $n=6$ for MMP-9, MMP-9 E402A and buffer
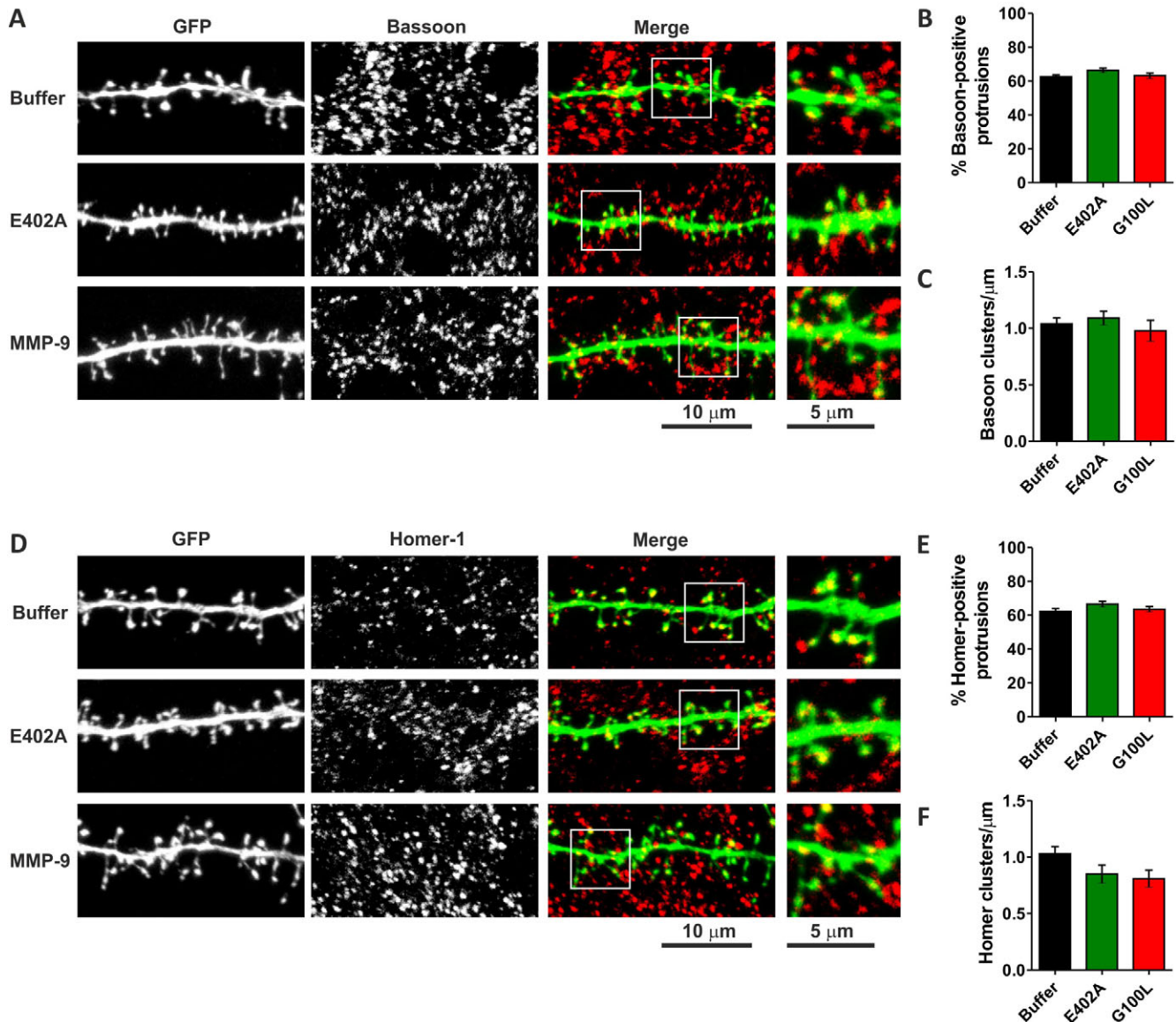
Fig. 5. MMP-9 enzymatic activity does not change the localization and abundance of synaptic markers. A dissociated hippocampal culture was transfected with plasmid caring eGFP under the β-actin promoter and, after reaching 15 DIV, cells were incubated for 90 minutes with 400 ng/ml of MMP-9 or inactive MMP-9 E402A, or buffer. Cells were fixed and stained for bassoon. (**A**) Examples of dendrites in GFP-expressing neurons, which were stained for bassoon after treatment with buffer, MMP-9 E402A or MMP-9. The furthest right-hand panel shows a magnification of the merge panels. (**B**) Mean ($\pm$ s.e.m.) percentage of bassoon-positive protrusions. (**C**) Density of bassoon clusters in the examined GFP-positive dendrites. (**D**) Examples of dendrites from GFP-expressing neurons that were stained for homer-1 after treatment with buffer, MMP-9 E402A or MMP-9. The furthest right-hand panel shows a magnification of the merged panel. (**E**) Mean ($\pm$ s.e.m.) percentage of homer-1-positive protrusions. (**F**) Density of homer-1 clusters in the examined GFP-positive dendrites.

treatment, respectively; $P<0.05$, unpaired Student's t-test, Fig. 6A,C). The MMP-9-induced slowdown of the mEPSC decay phase with respect to buffer or MMP-9-E402A-treated groups is particularly clear in the cumulative distribution of the decay time constants (Fig. 6D). Treatment with MMP-9 (or with MMP-9 E402A) for up to 90 minutes had no effect on mEPSC onset kinetics (data not shown).

The MMP-9 enzymatic activity influences spine morphology through engagement of integrin β1 subunit

It has been shown previously that MMP-9 can exert its function in neurons through engaging the integrin β1 subunit (Michaluk et al.,

2009; Nagy et al., 2006; Wang et al., 2008) and that integrins are involved in spine regulation (Bourgin et al., 2007; Shi and Ethell, 2006). Therefore, we decided to block the function of integrin β1 with a specific antibody and determine whether this would affect the action of MMP-9 on spine morphology. Dissociated hippocampal cultures were pretreated with either anti-integrin-β1 antibody or an isotype antibody (IgM), as a control, and were later incubated with either MMP-9 or MMP-9 E402A for 30 minutes (Fig. 7A). We did not observe any significant differences in spine density between the analysed groups (mean with IgM plus MMP-9 E402A, 0.7981 ± 0.0362 μm^{-1}, $n=16$ cells; mean with IgM plus MMP-9, 0.733 ± 0.041 μm^{-1}, $n=17$ cells; mean with anti-integrin-
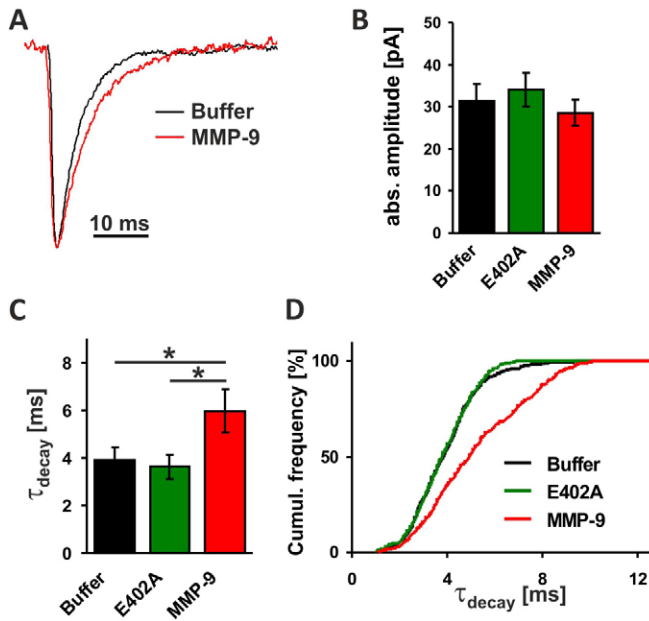
Fig. 6. MMP-9 enzymatic activity influences the kinetics of the synaptic current. (**A**) Example of normalized and superimposed typical mEPSCs recorded in control conditions (black) and after 90 minutes of treatment with MMP-9 (red). (**B**) Mean (absolute; ± s.e.m.) values of mEPSCs amplitudes recorded after 90 minutes of treatment with buffer, MMP-9 E402A or MMP-9. (**C**) mEPSC deactivation time constant (τ_{decay}) (mean ± s.e.m.) for currents recorded after 90 minutes of treatment with buffer, MMP-9 E402A or MMP-9. (**D**) Cumulative distribution of mEPSC time constants for currents recorded after 90 minutes of treatment with buffer, MMP-9 E402A or MMP-9. Cumulative distributions were constructed with data obtained from all cells included in the statistics but each cell is represented by an equal number (100) of mEPSCs.

β1 antibody and MMP-9 E402A, 0.8492 ± 0.04130 μm^{-1}, $n=16$ cells, mean with anti-integrin-β1 antibody and MMP-9, 0.8279 ± 0.05236 μm^{-1}, $n=15$ cells) (Fig. 7B). Two-way ANOVA did not reveal any significant differences for the antibody factor ($F=2.91$, $P=0.093$), for the MMP-9 factor ($F=1.02$, $P=0.32$) or for the interaction of both ($F=0.26$, $P=0.61$). Anti-integrin antibody did not influence spine shape parameter in the presence of inactive MMP-9 E402A in comparison with in the presence of isotype antibody (mean with anti-integrin-β1 antibody and MMP-9 E402A, 2.14 ± 0.045, $n=16$ cells; mean with IgM plus MMP-9, 2.21 ± 0.041, $n=16$ cells); however, it completely abolished the increase in the shape parameter caused by MMP-9 (mean with IgM plus MMP-9, 2.51 ± 0.065, $n=17$ cells; mean with anti-integrin-β1 antibody and MMP-9, 2.18 ± 0.061, $n=15$ cells) (Fig. 7C,D). Two-way ANOVA reached significance for the antibody factor ($F=13.3$, $P=0.0006$), for the MMP-9 factor ($F=9.59$, $P=0.003$) and moreover for interaction of both ($F=6.05$, $P=0.017$). Post-hoc Tukey's analysis revealed significant differences for IgM plus MMP-9 E402A compared with IgM plus MMP-9 ($P=0.0011$); anti-integrin-β1 antibody and MMP-9 compared with IgM plus MMP-9 ($P=0.00048$) and for anti-integrin-β1 antibody plus MMP-9 E402A compared with IgM plus MMP-9 ($P=0.0002$).

Discussion

Using three independent neuronal models (one in vivo and two in vitro) we show that excessive MMP-9 drives dendritic spines to change their shape towards being longer and thinner, which was characterized by an increase in a shape parameter (length:width). Moreover, we show that this process is mediated through integrin β1, as its blockade with a specific antibody abolished the effect on spine morphology caused by MMP-9. Furthermore, we provide evidence that changes in spine morphology can be

Fig. 7. MMP-9 enzymatic activity influences spine morphology through the integrin β1 subunit. (**A**) Representative images of two-week-old neurons in dissociated culture expressing eGFP preincubated with anti-integrin-β1 antibody (β$_1$Ab) or isotype antibody as a control (IgM) and later treated for 30 minutes with either MMP-9 or MMP-9 E402A as a control. (**B**) Mean (± s.e.m.) of protrusion density. Two-way ANOVA did not reveal any significant differences for antibody factor ($F=2.91$; $P=0.093$), for MMP-9 factor ($F=1.02$; $P=0.32$) or for the interaction of both ($F=0.26$; $P=0.61$). (**C**) Mean (± s.e.m.) of the shape parameter (length/width). Treatment with MMP-9 in the presence of IgM causes an increase in the shape parameter, but preincubation with β$_1$Ab completely abolishes this effect. Two-way ANOVA reached significance for antibody factor ($F=13.3$; $P=0.0006$), for MMP-9 factor ($F=9.59$; $P=0.003$) and, moreover, for the interaction of both ($F=6.05$; $P=0.017$). Post-hoc Tukey's analysis revealed significant differences for IgM + E402A compared with IgM + MMP-9 ($P=0.0011$); β$_1$Ab + MMP-9 compared with IgM + MMP-9 ($P=0.00048$) and for β$_1$Ab + E402A compared with IgM + MMP-9 ($P=0.0002$). (**D**) Cumulative frequency graph of the shape parameter (length/width) of spines in all groups.

associated with modifications of the decay time of synaptic currents.

To study the influence MMP-9 on spines in vivo we used transgenic rats overexpressing autoactivating MMP-9 under the control of the synapsin I promoter. In comparison with control (WT rats), intensified MMP-9 activity caused an increase in the spine length:width ratio. Furthermore, we confirmed our light microscopy data with electron microscopy, demonstrating clearly that there is an increase in the largest spine category, thin spines, at the expense of mushroom spines, which decrease as a percentage of the total spine complement. Interestingly, Bilousova et al. have observed a decreased spine-head area and increased length of spines in CA1 and CA3 regions of the hippocampus in *Fmr1*-knockout mouse, which among various pathological features overexpresses MMP-9 (Bilousova et al., 2009). This phenotype was rescued by treatment with minocycline, a tetracycline derivative that, among other effects, decreases the expression and activity of MMP-9 (Yao et al., 2004).

To avoid subjective discrimination between spines and filopodia we utilized a shape parameter defined as the ratio of the length to the maximal width of the spine. We decided to do this because there is no coherent definition of a filopodium and many research groups use different shape parameters to distinguish between these structures and, moreover, there is also no clear functional criterion of filopodia.

For our studies, we have produced a recombinant autoactivating mutant of MMP-9, as well as its inactive form MMP-9 E402A, and characterized both proteins, which were then used in hippocampal cultures. These new experimental tools allowed us to address, for the first time, directly the issue of whether enzymatic activity and not just protein–protein interactions are responsible for the effect of MMP-9 on spines. This was important because MMP-9 has several structural protein domains and has been shown to have biological activity in the absence of enzymatic activity (Ezhilarasan et al., 2009; Redondo-Munoz et al., 2010). Furthermore, it has been reported that MMP-9 is capable of binding many surface proteins, such as integrins (Bjorklund et al., 2004; Redondo-Munoz et al., 2008; Stefanidakis et al., 2003), LRP-1 (Van den Steen et al., 2006) and CD44 (Bourguignon et al., 1998). We demonstrated clearly that lack of enzymatic activity renders the MMP-9 inactive mutant MMP-9 E402A incapable of affecting either spine morphology or changing the shape parameter in hippocampal cultures.

Initially, the effects of the recombinant MMP-9 proteins were demonstrated in live organotypic hippocampal cultures. Wang et al. (Wang et al., 2008) also noted the effect of application of recombinant MMP-9 on spine morphology, namely on increasing spine-head volume. However, no detailed analyses of the spine geometry were provided in that study. To extend further our observations we also employed dissociated hippocampal cultures, which in this case are more amenable to experimental manipulation. Incubation of neurons at 15 DIV with recombinant MMP-9 also caused a significant increase in length:width parameter, which was notable after only 30 minutes of incubation. This result is in agreement with previous observations of Bilousova et al. (Bilousova et al., 2009), who also applied recombinant MMP-9 for 1 hour in dissociated hippocampal culture and demonstrated an increase in the number of filopodia-like long spines with small heads and a concomitant decrease in the number of mushroom-shaped short spines with large heads. Furthermore, it was recently shown that 6 hours of treatment with 5 µM NMDA caused an increase in spine number, and the appearance of new small spines

and maturation of existing spines, which was blocked by both the MMP-2 and MMP-9 inhibitor, and by the knockout of ICAM-5, the presumed MMP-2 and MMP-9 substrate (Tian et al., 2007). The proposed model assumes that MMP-2 and/or MMP-9 enzymatic activity, upon neuronal stimulation, leads to maturation of spines and elongation of filopodia (Tian et al., 2007). Interestingly, the recent findings of Conant et al. (Conant et al., 2010) support the notion that ICAM-5 cleavage by MMPs (also including MMP-3 and MMP-7) can occur as early as 15 minutes after neuronal stimulation by either NMDA treatment or induction of LTP.

We have also shown that the changes in spine morphology induced by MMP-9 treatment are not accompanied by significant changes in the abundance and localization of the presynaptic marker bassoon, which suggests that MMP-9 activity does not affect synaptic contacts of dendritic protrusions. Moreover, we observed that incubation of neurons with MMP-9 caused a slowing of the mEPSC decay phase (Fig. 6A–D) without affecting the absolute amplitude. The increase in decay time is intriguing, as neuronal development comprises both conversion of spine shape (from filopodial into mushroom-like) and an increase in synaptic currents (Cathala et al., 2005; Wall et al., 2002). Thus, the appearance of filopodia and slowing of mEPSCs might suggest an MMP-9-induced 'juvenalization' of glutamatergic synapses in our model. However, the precise mechanism of mEPSC slowing described here is not clear. Several potential processes might underlie the change in the timecourse of mEPSCs, including a subunit switch (Kumar et al., 2002), lateral receptor mobility (Heine et al., 2008), endocytosis or exocytosis of receptors (Lee et al., 2004), changes in synapse geometry (Barbour et al., 1994; Cathala et al., 2005) and post-translational modulation of synaptic receptors (Lee, 2006). Notably, Cathala et al. (Cathala et al., 2005) have attributed the developmental speeding of glutamatergic EPSCs, to changes in the synapse geometry, a mechanism that might be consistent with the changes in spine shape and mEPSC kinetics that we observed here. However, it should be stressed that the induction of filopodial spine shape by MMP-9, as described here, need not be the only mechanism whereby these enzymes could affect the glutamatergic synapse. For instance, MMPs could change the synaptic cleft geometry, the relative localization of releasing sites and of postsynaptic densities and alter the immediate surrounding of the synapse (thus affecting the diffusion of the agonist to the receptors), giving rise to a change in synaptic glutamate transients, thereby altering mEPSC kinetics. Moreover, the fact that 30 minutes of treatment with MMP-9 was sufficient to induce a significant alteration in spine shape, whereas 90 minutes were needed for MMP-9 to induce a change in the mEPSC kinetics, suggests that additional factors, other than spine geometry, might also be involved. Further studies are needed to elucidate the extent to which MMP-9 treatment modulates the shape and function of glutamatergic synapses by either common or separate mechanisms.

Finally, we have shown that the influence of MMP-9 on spines depends on integrin β1 activation, which agrees with previous reports that MMP-9 acts through this integrin subunit (Michaluk et al., 2009; Nagy et al., 2006; Wang et al., 2008) and that MMP-9 can bind integrins (Redondo-Munoz et al., 2008; Rolli et al., 2003; Stefanidakis et al., 2003). The influence of integrins on spine morphology reported previously agrees with those results (Shi and Ethell, 2006). In particular, RGD peptides that mimic integrin ligands, and can stimulate integrin signalling, can cause elongation of spines and formation of new filopodia (Shi and

Ethell, 2006). We suggest that all of these results could be interpreted in the following way: MMP-9, by virtue of its proteolytic activity, cleaves some, yet to be defined, ECM component or cell adhesion molecule and thus releases cryptic ligand-binding integrins. MMP-9 has been shown previously to produce such ligands in other tissues (Dityatev et al., 2010; Van den Steen et al., 2000; Xu et al., 2001).

In conclusion, our data, considered together with those from several recent studies, strongly indicate that MMP-9 can be functionally involved in synaptic remodelling. Such an activity might explain the physiological role of MMP-9 in LTP, as well as in learning and memory (Meighan et al., 2006; Nagy et al., 2006; Okulski et al., 2007) and in pathological conditions implicating neuronal plasticity (e.g. epilepsy and drug addiction) (see Kim et al., 2009; Mash et al., 2007; Rivera et al., 2010; Samochowiec et al., 2010; Takacs et al., 2010; Wilczynski et al., 2008; Yamada, 2008).

Materials and Methods

Transgenic rats

All animal experiments were performed according to approved guidelines. Transgenic rats overexpressing autoactivating MMP-9 under the control of the synapsin 1 promoter (Wilczynski et al., 2008) were injected with pentobarbital (200 mg per kg of body weight; intraperitoneal injection) and perfused transcardially, first with PBS (15 ml per rat) and then with 4% paraformaldehyde (PFA, 60 ml per rat). Brains were cut out into 300-μm-thick vibratome slices. Random dendrite labelling with a gene gun, using 1.6 μm tungsten particles (BioRad) coated with propelled lipophilic fluorescent dye (DiI; Invitrogen), was performed for the spine classification. Slices were incubated in 1.5% PFA for 48 hours. Images of secondary apical dendrites (50 μm–200 μm) from the cell soma of the CA1 field of hippocampus were acquired under 561-nm fluorescent illumination using a confocal microscope (63$\times$ objective, 1.4 NA) at a pixel resolution of 1024×1024 with a 3.43 zoom, which resulted in a 72-nm pixel size. Spines were measured and analysed using ImageJ software (NIH). There were 4 animals ($n=4$ rats) in each group for the spine analyses. From each of the animals, at least 200 spines were analysed, which were made at least two neurons per animal and two dendrites of an overall dendritic length of 250 μm per neuron. This result was from more than 1200 spines measured for both wild-type and transgenic rats.

Transmission electron microscopy

Brains for three-dimensional analyses were cut into 50-μm-thick vibratome slices (VT1000; Leica, Milton Keynes, UK) and transferred to 2.5% glutaraldehyde in 0.1 M PBS. After washing with buffer, the tissue was osmicated in 2% osmium tetroxide and dehydrated in graded aqueous solutions of ethanol from 40 to 96% (each for 10 minutes) and then 100% acetone (three changes, each for 10 minutes). Specimens were infiltrated with a mixture of 50% epoxy resin and 50% pure acetone for 30 minutes at room temperature. Each slice was placed on an Aclar film and covered with a capsule containing pure epoxy resin (Epon 812, Araldite M epoxy resins) for 1 hour at 60℃ and polymerized overnight at 80℃. A trapezoid area on the surface of the blocks containing hippocampus was prepared with a glass knife, with one side of 200–250 μm in length, which included the whole CA1 region. This procedure is illustrated in Popov et al. (Popov et al., 2005; Popov et al., 2004). Serial sections of grey and white colour (60–70 nm) were cut with a Diatome diamond knife and allowed to form a ribbon on the surface of a water and ethanol solution (2–5% ethanol in water) in the knife bath and collected using Pioloform-coated slot copper grids (each series comprises up to 100 serial sections). Sections were counterstained with saturated ethanolic uranyl acetate, followed by lead citrate. Finally sections were imaged in stratum radiatum area of CA1 using an AMT XR40 4 megapixel camera mounted onto a JEOL 1010 electron microscope.

Digital reconstructive analysis

Serial sections were aligned as JPEG images (software available from http://synapses.clm.utexas.edu/). Alignments were made with full-field images. Stereological analysis was performed as described previously (Harris, 1994; Popov et al., 2004), with tissue volumes of ~500–800 μm^3. Because synapse density is markedly influenced by elements occurring non-uniformly in the sample areas (i.e. myelinated axons, cell bodies, non-spiny interneuron dendrites and large dendrites with section profiles that are >0.94 μm^2), the areas of these elements were measured and subtracted from the sample areas to obtain the homogeneous neuropil area to avoid bias in the data obtained, as described previously (Harris, 1994; Popov et al., 2004). Synaptic densities were expressed as the number of synapses [identified through postsynaptic densities (PSDs) and the presence of at least two presynaptic vesicles] per 100 μm^3 of tissue. Synaptic densities were

expressed as the number of synapses (identified through PSDs and the presence of at least two presynaptic vesicles) per 100 μm^3 of tissue. Spines and synapses were categorized as described previously (Harris et al., 1992; Peters and Kaiserman-Abramof, 1970). We thus distinguished three spine categories: mushroom, where the spine head is large and considerably in excess of the spine neck diameter; thin, where the height is usually several times in excess of the width; and stubby, where the spine protrudes only slightly from the dendritic shaft. Shaft synapses are a fourth category where the synapse contacts directly the dendritic shaft. There were three animals in each group for the three-dimensional analyses, which were made from the stratum radiatum of CA1; 25 thin and 25 mushroom spines were reconstructed to analyse spine volume, surface area and curvature of the PSD, as described previously (Popov et al., 2008). The volume and surface area of PSDs on these reconstructed spines were also analysed. All data were averaged to receive 1 mean per animal for each parameter and all statistics for three-dimensional analyses were calculated using this data (one value per animal). The curvature of dendritic spines was measures as described previously (Popov et al., 2008). All data from digital reconstructive analysis was evaluated to give 1 value for each individual animal in each data set. Three-dimensional reconstructions were exported to 3D-Studio-Max 8 software for rendering and subsequent rotation to display the optimal views of the reconstructed structures.

Recombinant autoactivating MMP-9 and inactive MMP-9 E402A

Expression of the previously described (Fisher et al., 2002) auto-activating mutant of MMP-9 was performed using the Bac-to-Bac Baculovirus expression system, according to the manufacturer's instructions (Invitrogen). Briefly, the MMP-9 G100L mutant (a gift from Katherine Fisher, Pfizer, Groton, PA) was cloned into pFastBac1, and the resulting recombinant plasmid was used to transform DH10Bac competent cells. Colonies that performed transposition of recombinant plasmid fragment into bacmid DNA were identified by blue–white selection, and recombinant bacmid was isolated and verified by PCR. The Sf21 insect cells were transfected with recombinant bacmid using Cellfectin reagent (Invitrogen) to obtain recombinant baculovirus. After amplification and titration of the recombinant baculovirus, High-Five cells were infected and incubated in the Sf-900IISFM serum-free medium (Invitrogen). Conditioned medium was collected for analysis of expression by gel zymography. At 24, 48 and 72 hours after infection, medium was collected and an equal volume was tested by gel zymography. The highest expression level was observed at 48 hours post infection (data not shown). Thus, the cell medium harvested 48 hours after the infection with baculovirus was used for purification of recombinant autoactivating mutant of MMP-9 by affinity chromatography with gelatin–Sepharose 4B (GE Healthcare) as previously described (Sadatmansoori et al., 2001). Protein concentrations in the collected fractions were measured using Bradford reagent (Sigma). The recombinant inactive mutant MMP-9 E402A was generated using QuikChange (Stratagene) according to the manufacturer's instructions. The point mutation changing glutamate 402 into alanine in the catalytic centre of human MMP-9 was inserted by PCR using a pair of primers: 5′-TGGCGGCGCATGCGTT-CGGCCACGC-3′ and 5′-GCGTGGCCGAACGCATGCGCCGCCA-3′. Next MMP-9 E402A was cloned into the pFastBac1 vector, and expression and purification of protein was performed exactly as described for MMP-9. The enzymatic activity of purified MMP-9 and MMP-9 E402A was checked with the EnzCheck gelatinase/collagenase assay kit (Invitrogen) according to the manufacturer's instructions.

Western blotting

Samples were subjected to SDS-PAGE (8% gels) and electrotransferred onto polyvinylidene difluoride membrane (Immobilon-P, Millipore), which were blocked for 2 hours at room temperataure with 10% (w/v) dried non-fat milk powder in Tris-buffered saline with 0.1% Tween 20 (TBS-T). After blocking, the membranes were incubated at 4℃ overnight with rabbit anti-human-MMP-9 antibody (Abcam, # ab52496) diluted in 5% (w/v) dried non-fat milk powder in TBS-T. Membranes were then incubated for 2 hours at room temperature with horseradish-peroxidase-labelled secondary antibody diluted 1:10,000 in 5% dried non-fat milk powder in TBS-T. After washing, the peroxidase activity was visualized with ECLplus reagent (GE Healthcare).

Gel zymography

Samples of culture medium were mixed with 33 SDS sample buffer without DTT and subjected to SDS-PAGE (8% gels containing 2 mg/ml gelatine). The gels were then washed twice with 2.5% Triton X-100 for 30 minutes at room temperature and incubated overnight in developing buffer (50 mM Tris-HCl pH 7.5, 10 mM CaCl$_2$, 1 μM ZnCl$_2$, 1% Triton X-100 and 0.02% NaN$_3$) at 37℃ with moderate shaking. Gels were stained with Coomassie Brilliant Blue and briefly destained.

Hippocampal organotypic cultures and live imaging

Transverse hippocampal organotypic cultures were prepared as described previously (Stoppini et al., 1991). Briefly, 400-μm-thick hippocampal slices were cut from 6- to 7-day-old rats and maintained for 11–18 days at 33℃ under an humidified 5% CO$_2$

atmosphere on Millipore inserts in culture medium (MEM plus HEPES, 25% horse serum and 25% Hanks solution). After 8 DIV cultures were transfected with either pcDNA3.1-eGFP or a pCX-mRFP1 using a biolistic method (Helios Gene Gun, Bio-Rad) and were used for experiments 3 days after transfection (De Roo et al., 2008a). Brief imaging sessions were carried out with an Olympus Fluoview 300 system coupled to a single photon laser. We focused on secondary or tertiary apical dendrites from CA1 field of hippocampus using a 403 objective (0.8 NA) and 103 digital zoom (final resolution 25 pixel size; steps between scans of 0.4 μm). Z-stacks were analysed manually using ImageJ software (NIH).

Dissociated hippocampal cultures

Dissociated hippocampal cultures from P0 (postnatal day 0) Wistar rats were prepared as described below. Brains were removed and hippocampi were isolated on ice in dissociation medium DM; 81.8 mM Na_2SO_4, 30 mM K_2SO_4, 5.8 mM $MgCl_2$, 0.25 mM $CaCl_2$, 1 mM HEPES pH 7.4, 20 mM glucose; 1 mM kynureic acid; 0.001% Phenol Red), hippocampi were later incubated twice for 15 minutes at 37℃ with 100 units of papain (Worthington, NY) in DM and rinsed three times in DM and subsequently three times in plating medium [MEM, 10% fetal bovine serum (FBS) and 1% penicilin-streptomycin]. Hippocampi were triturated in plating medium until no clumps were visible and cells were diluted 1:10 in OptiMEM (Invitrogen), centrifuged for 10 minutes at room temperature, at 208.5 g. The resulting cell pellet was suspended in plating medium, cells were counted and plated at density 120,000 cells per 18-mm-diameter coverslip (Assistent, Germany) coated with 1 mg/ml poly-L-lysine (Sigma) and 2.5 μg/ml laminin (Roche). At 3 hours after plating medium was exchanged for maintenance medium (Neurobasal-A without Phenol Red, 2% B-27 supplement, 1% penicillin-streptomycin, 0.5 mM glutamine, 12.5 μM glutamate, 25 μM β-mercaptoethanol) and cells were kept at 37℃, under a humidified 5% CO_2 atmosphere for 2 weeks. All experiments were performed at 14–19 days in vitro (DIV). Cells were transfected using Effectene (Qiagen), according to the manufacturer's protocol, at 10 DIV with plasmid carrying eGFP under the control of the β-actin promoter.

Cell stimulation

Cells were incubated for 30–90 minutes with 400 ng/ml of recombinant MMP-9 or MMP-9 E402A in maintenance medium or the buffer (50 mM Tris-HCl pH 7.5, 400 mM NaCl, 10 mM $CaCl_2$ and 2% DMSO) used for elution of recombinant proteins from the affinity column, which was diluted at least 1:125 in the maintenance medium, so the final concentration of DMSO in the culture did not exceed 0.016%. As indicated, cells were also incubated overnight with anti-CD29 (integrin β1 chain) antibody (BD Pharmingen, no. 555002) or isotype antibody (IgM; BD Pharmingen no. 553957) at a final concentration of 40 μg/ml.

Immunostaining and confocal microscopy

Cells were fixed for 10 minutes at room temperature with 4% PFA, washed with PBS, permeabilized for 7 minutes with 0.1% Triton X-100 in PBS and blocked for 1 hour at room temperature with 10% normal goat serum in PBS. After blocking, cells were incubated overnight with mouse anti-GFP antibody (Millipore # MAB3580) and rabbit anti-bassoon antibody (Synaptic Systems no. 141003), and guinea-pig anti-homer-1 antibody (Synaptic systems no. 160004), and then were washed and incubated with fluorescent (Alexa-Fluor-488-, -568 or -647-conjugated) secondary anti-rabbit-IgG antibody (Invitrogen) for 40 minutes at room temperature, washed and mounted. Fluorescent specimens were examined under a confocal microscope (TCS SP2; Leica) equipped with a 633 1.32 NA oil immersion objective using the 488 nm line of an argon laser (for excitation of Alexa Fluor 488), the 633 nm line of a helium-neon laser (for excitation of Alexa Fluor 647) and the 543 nm line of a helium-neon laser (for excitation of Alexa Fluor 568) of an at a pixel resolution of 2048 × 2048 and 1.653 optical zoom. The resulting pixel size was 70.45 nm. The Z-stacks of optical slices were acquired in 0.2 μm steps. The sum of Z-stacks of secondary or higher order dendrites (mostly of pyramidal neurons) were analysed with ImageJ software (NIH). We discarded from the analyses all objects (protrusions) with an area smaller than 0.2 μm² owing to the planar resolution of confocal setup. Colocalization of the synaptic marker with dendritic protrusions was determined manually using merged images. The percentage of clusters colocalized with protrusions relative to total was then calculated (Verpelli et al., 2010). All measurements were expressed as mean ± s.e.m.

Electrophysiology

Miniature excitatory postsynaptic currents (mEPSC) were recorded in the whole-cell configuration of the patch-clamp technique at a membrane voltage of –70 mV, using the Axopatch 200B amplifier (Molecular Devices Corporation, Sunnyvale, CA). Signals were low-pass filtered at 5 kHz and acquired at 50 kHz in the gap-free mode using the analogue-to-digital converter Digidata 1440A (Molecular Devices Corporation). The intrapipette solution contained: 137 mM CsCl, 1 mM $CaCl_2$, 2 mM $MgCl_2$, 11 mM BAPTA (tetra cesium salt), 2 mM ATP and 10 mM HEPES pH 7.2 with CsOH. The composition of the external solution was: 137 mM NaCl, 5 mM KCl, 2 mM $CaCl_2$, 1 mM $MgCl_2$, 20 mM glucose and 10 mM HEPES pH 7.2 with NaOH. mEPSCs were recorded in the presence of 1 μM tetrodotoxin (TTX) to suppress neuronal excitability and 5 μM SR-95531 was added to the external solution to block the GABAergic synaptic transmission. The presence of magnesium (2 mM) in the external saline and the highly negative membrane voltage (–70 mV) were expected to eliminate the NMDA-receptor-mediated component of synaptic currents. All recordings were performed at room temperature (21–24℃). Chemicals were from Sigma except for TTX (LaToxan, France). The mEPSCs decaying phase was fitted to a single exponential function $y(t)=A \exp(-t/\tau_{decay})$, where A is the amplitude and τ_{decay} is the decay time constant. To assess the impact of MMP-9 on mEPSCs, neurons were incubated for up to 90 minutes in culture medium with recombinant MMP-9 at concentration of 400 ng/ml. Control recordings were performed in parallel on two groups of neurons from the same preparation: one treated for the same time duration with respective volume of MMP-9 dilution buffer and the second group treated for the same time and with the same amount of enzymatically inactive MMP-9 E402A. The effect of MMP-9 was assessed for neurons treated for 30, 60 and 90 minutes.

Statistics

Data were tested for normal distribution using the Kolmogorov–Smirnov normality test and because all data passed that test, they were expressed as means ± s.e.m. Groups were compared using unpaired Student's t-tests and if the number of groups was larger than two, we used a one-way or two-way ANOVA and a post-hoc Tukey's test. The number of animals and/or the number of cells (n) used for statistical evaluation of the means ± s.e.m values is provided, after the corresponding mean value for each analysed group, in the Results section.

References

Asahi, M., Asahi, K., Jung, J. C., del Zoppo, G. J., Fini, M. E. and Lo, E. H. (2000). Role for matrix metalloproteinase 9 after focal cerebral ischemia: effects of gene knockout and enzyme inhibition with BB-94. J. Cereb. Blood Flow Metab. **20**, 1681-1689.

Barbour, B., Keller, B. U., Llano, I. and Marty, A. (1994). Prolonged presence of glutamate during excitatory synaptic transmission to cerebellar Purkinje cells. Neuron **12**, 1331-1343.

Bilousova, T. V., Rusakov, D. A., Ethell, D. W. and Ethell, I. M. (2006). Matrix metalloproteinase-7 disrupts dendritic spines in hippocampal neurons through NMDA receptor activation. J. Neurochem. **97**, 44-56.

Bilousova, T. V., Dansie, L., Ngo, M., Aye, J., Charles, J. R., Ethell, D. W. and Ethell, I. M. (2009). Minocycline promotes dendritic spine maturation and improves behavioural performance in the fragile X mouse model. J. Med. Genet. **46**, 94-102.

Bjorklund, M., Heikkila, P. and Koivunen, E. (2004). Peptide inhibition of catalytic and noncatalytic activities of matrix metalloproteinase-9 blocks tumor cell migration and invasion. J. Biol. Chem. **279**, 29589-29597.

Bourgin, C., Murai, K. K., Richter, M. and Pasquale, E. B. (2007). The EphA4 receptor regulates dendritic spine remodeling by affecting beta1-integrin signaling pathways. J. Cell Biol. **178**, 1295-1307.

Bourguignon, L. Y., Gunja-Smith, Z., Iida, N., Zhu, H. B., Young, L. J., Muller, W. J. and Cardiff, R. D. (1998). CD44v(3,8-10) is involved in cytoskeleton-mediated tumor cell migration and matrix metalloproteinase (MMP-9) association in metastatic breast cancer cells. J. Cell. Physiol. **176**, 206-215.

Brown, T. E., Wilson, A. R., Cocking, D. L. and Sorg, B. A. (2009). Inhibition of matrix metalloproteinase activity disrupts reconsolidation but not consolidation of a fear memory. Neurobiol. Learn. Mem. **91**, 66-72.

Cathala, L., Holderith, N. B., Nusser, Z., DiGregorio, D. A. and Cull-Candy, S. G. (2005). Changes in synaptic structure underlie the developmental speeding of AMPA receptor-mediated EPSCs. Nat. Neurosci. **8**, 1310-1318.

Chklovskii, D. B., Mel, B. W. and Svoboda, K. (2004). Cortical rewiring and information storage. Nature **431**, 782-788.

Conant, K., Wang, Y., Szklarczyk, A., Dudak, A., Mattson, M. P. and Lim, S. T. (2010). Matrix metalloproteinase-dependent shedding of intercellular adhesion molecule-5 occurs with long-term potentiation. Neuroscience **166**, 508-521.

De Roo, M., Klauser, P., Mendez, P., Poglia, L. and Muller, D. (2008a). Activity-dependent PSD formation and stabilization of newly formed spines in hippocampal slice cultures. Cereb. Cortex **18**, 151-161.

De Roo, M., Klauser, P. and Muller, D. (2008b). LTP promotes a selective long-term stabilization and clustering of dendritic spines. *PLoS Biol.* **6**, e219.

Dityatev, A., Schachner, M. and Sonderegger, P. (2010). The dual role of the extracellular matrix in synaptic plasticity and homeostasis. *Nat. Rev. Neurosci.* **11**, 735-746.

Ezhilarasan, R., Jadhav, U., Mohanam, I., Rao, J. S., Gujrati, M. and Mohanam, S. (2009). The hemopexin domain of MMP-9 inhibits angiogenesis and retards the growth of intracranial glioblastoma xenograft in nude mice. *Int. J. Cancer* **124**, 306-315.

Fisher, K. E., Fei, Q., Laird, E. R., Stock, J. L., Allen, M. R., Sahagan, B. G. and Strick, C. A. (2002). Engineering autoactivating forms of matrix metalloproteinase-9 and expression of the active enzyme in cultured cells and transgenic mouse brain. *Biochemistry* **41**, 8289-8297.

Grabrucker, A., Vaida, B., Bockmann, J. and Boeckers, T. M. (2009). Synaptogenesis of hippocampal neurons in primary cell culture. *Cell Tissue Res.* **338**, 333-341.

Gu, Z., Kaul, M., Yan, B., Kridel, S. J., Cui, J., Strongin, A., Smith, J. W., Liddington, R. C. and Lipton, S. A. (2002). S-nitrosylation of matrix metalloproteinases: signaling pathway to neuronal cell death. *Science* **297**, 1186-1190.

Harris, K. M. (1994). Serial electron microscopy as an alternative or compliment to confocal microscopy for the study of synapses and dendritic spines in the central nervous system. In *Three-Dimensional Confocal Microscopy, Volume Investigation Of Biological Specimens* (ed. J. K. Stevens, L. R. Mills and J. E. Trogadis), pp. 421-445. New York: Academic Press.

Harris, K. M., Jensen, F. E. and Tsao, B. (1992). Three-dimensional structure of dendritic spines and synapses in rat hippocampus (CA1) at postnatal day 15 and adult ages: implications for the maturation of synaptic physiology and long-term potentiation. *J. Neurosci.* **12**, 2685-2705.

Heine, M., Groc, L., Frischknecht, R., Beique, J. C., Lounis, B., Rumbaugh, G., Huganir, R. L., Cognet, L. and Choquet, D. (2008). Surface mobility of postsynaptic AMPARs tunes synaptic transmission. *Science* **320**, 201-205.

Holtmaat, A. and Svoboda, K. (2009). Experience-dependent structural synaptic plasticity in the mammalian brain. *Nat. Rev. Neurosci.* **10**, 647-658.

Holtmaat, A., Wilbrecht, L., Knott, G. W., Welker, E. and Svoboda, K. (2006). Experience-dependent and cell-type-specific spine growth in the neocortex. *Nature* **441**, 979-983.

Kim, G. W., Kim, H. J., Cho, K. J., Kim, H. W., Cho, Y. J. and Lee, B. I. (2009). The role of MMP-9 in integrin-mediated hippocampal cell death after pilocarpine-induced status epilepticus. *Neurobiol. Dis.* **36**, 169-180.

Konopka, W., Kiryk, A., Novak, M., Herwerth, M., Parkitna, J. R., Wawrzyniak, M., Kowarsch, A., Michaluk, P., Dzwonek, J., Arnsperger, T. et al. (2010). MicroRNA loss enhances learning and memory in mice. *J. Neurosci.* **30**, 14835-14842.

Kumar, S. S., Bacci, A., Kharazia, V. and Huguenard, J. R. (2002). A developmental switch of AMPA receptor subunits in neocortical pyramidal neurons. *J. Neurosci.* **22**, 3005-3015.

Lee, H. K. (2006). Synaptic plasticity and phosphorylation. *Pharmacol. Ther.* **112**, 810-832.

Lee, S. H., Simonetta, A. and Sheng, M. (2004). Subunit rules governing the sorting of internalized AMPA receptors in hippocampal neurons. *Neuron* **43**, 221-236.

Mash, D. C., ffrench-Mullen, J., Adi, N., Qin, Y., Buck, A. and Pablo, J. (2007). Gene expression in human hippocampus from cocaine abusers identifies genes which regulate extracellular matrix remodeling. *PLoS ONE* **2**, e1187.

Matsuzaki, M., Honkura, N., Ellis-Davies, G. C. and Kasai, H. (2004). Structural basis of long-term potentiation in single dendritic spines. *Nature* **429**, 761-766.

Meighan, S. E., Meighan, P. C., Choudhury, P., Davis, C. J., Olson, M. L., Zornes, P. A., Wright, J. W. and Harding, J. W. (2006). Effects of extracellular matrix-degrading proteases matrix metalloproteinases 3 and 9 on spatial learning and synaptic plasticity. *J. Neurochem.* **96**, 1227-1241.

Michaluk, P., Mikasova, L., Groc, L., Frischknecht, R., Choquet, D. and Kaczmarek, L. (2009). Matrix metalloproteinase-9 controls NMDA receptor surface diffusion through integrin beta1 signaling. *J. Neurosci.* **29**, 6007-6012.

Mizoguchi, H., Yamada, K., Niwa, M., Mouri, A., Mizuno, T., Noda, Y., Nitta, A., Itohara, S., Banno, Y. and Nabeshima, T. (2007). Reduction of methamphetamine-induced sensitization and reward in matrix metalloproteinase-2 and -9-deficient mice. *J. Neurochem.* **100**, 1579-1588.

Moeller, M. L., Shi, Y., Reichardt, L. F. and Ethell, I. M. (2006). EphB receptors regulate dendritic spine morphogenesis through the recruitment/phosphorylation of focal adhesion kinase and RhoA activation. *J. Biol. Chem.* **281**, 1587-1598.

Moser, M. B., Trommald, M. and Andersen, P. (1994). An increase in dendritic spine density on hippocampal CA1 pyramidal cells following spatial learning in adult rats suggests the formation of new synapses. *Proc. Natl. Acad. Sci. USA* **91**, 12673-12675.

Mott, J. D. and Werb, Z. (2004). Regulation of matrix biology by matrix metalloproteinases. *Curr. Opin. Cell Biol.* **16**, 558-564.

Mysore, S. P., Tai, C. Y. and Schuman, E. M. (2007). Effects of N-cadherin disruption on spine morphological dynamics. *Front. Cell. Neurosci.* **1**, 1.

Nagy, V., Bozdagi, O., Matynia, A., Balcerzyk, M., Okulski, P., Dzwonek, J., Costa, R. M., Silva, A. J., Kaczmarek, L. and Huntley, G. W. (2006). Matrix metalloproteinase-9 is required for hippocampal late-phase long-term potentiation and memory. *J. Neurosci.* **26**, 1923-1934.

Niu, S., Yabut, O. and D'Arcangelo, G. (2008). The Reelin signaling pathway promotes dendritic spine development in hippocampal neurons. *J. Neurosci.* **28**, 10339-10348.

Okulski, P., Jay, T. M., Jaworski, J., Duniec, K., Dzwonek, J., Konopacki, F. A., Wilczynski, G. M., Sanchez-Capelo, A., Mallet, J. and Kaczmarek, L. (2007). TIMP-1 abolishes MMP-9-dependent long-lasting long-term potentiation in the prefrontal cortex. *Biol. Psychiatry* **62**, 359-362.

Peters, A. and Kaiserman-Abramof, I. R. (1970). The small pyramidal neuron of the rat cerebral cortex. The perikaryon, dendrites and spines. *Am. J. Anat.* **127**, 321-355.

Petrini, E. M., Lu, J., Cognet, L., Lounis, B., Ehlers, M. D. and Choquet, D. (2009). Endocytic trafficking and recycling maintain a pool of mobile surface AMPA receptors required for synaptic potentiation. *Neuron* **63**, 92-105.

Pizzorusso, T., Medini, P., Berardi, N., Chierzi, S., Fawcett, J. W. and Maffei, L. (2002). Reactivation of ocular dominance plasticity in the adult visual cortex. *Science* **298**, 1248-1251.

Popov, V. I., Davies, H. A., Rogachevsky, V. V., Patrushev, I. V., Errington, M. L., Gabbott, P. L., Bliss, T. V. and Stewart, M. G. (2004). Remodelling of synaptic morphology but unchanged synaptic density during late phase long-term potentiation (LTP): a serial section electron micrograph study in the dentate gyrus in the anaesthetised rat. *Neuroscience* **128**, 251-262.

Popov, V., Medvedev, N. I., Davies, H. A. and Stewart, M. G. (2005). Mitochondria form a filamentous reticular network in hippocampal dendrites but are present as discrete bodies in axons: a three-dimensional ultrastructural study. *J. Comp. Neurol.* **492**, 50-65.

Popov, V. I., Medvedev, N. I., Kraev, I. V., Gabbott, P. L., Davies, H. A., Lynch, M., Cowley, T. R., Berezin, V., Bock, E. and Stewart, M. G. (2008). A cell adhesion molecule mimetic, FGL peptide, induces alterations in synapse and dendritic spine structure in the dentate gyrus of aged rats: a three-dimensional ultrastructural study. *Eur. J. Neurosci.* **27**, 301-314.

Redondo-Munoz, J., Ugarte-Berzal, E., Garcia-Marco, J. A., del Cerro, M. H., Van den Steen, P. E., Opdenakker, G., Terol, M. J. and Garcia-Pardo, A. (2008). Alpha4beta1 integrin and 190-kDa CD44v constitute a cell surface docking complex for gelatinase B/MMP-9 in chronic leukemic but not in normal B cells. *Blood* **112**, 169-178.

Redondo-Munoz, J., Ugarte-Berzal, E., Terol, M. J., Van den Steen, P. E., Hernandez del Cerro, M., Roderfeld, M., Roeb, E., Opdenakker, G., Garcia-Marco, J. A. and Garcia-Pardo, A. (2010). Matrix metalloproteinase-9 promotes chronic lymphocytic leukemia b cell survival through its hemopexin domain. *Cancer Cell* **17**, 160-172.

Rivera, S., Khrestchatisky, M., Kaczmarek, L., Rosenberg, G. A. and Jaworski, D. M. (2010). Metzincin proteases and their inhibitors: foes or friends in nervous system physiology? *J. Neurosci.* **30**, 15337-15357.

Rolli, M., Fransvea, E., Pilch, J., Saven, A. and Felding-Habermann, B. (2003). Activated integrin alphavbeta3 cooperates with metalloproteinase MMP-9 in regulating migration of metastatic breast cancer cells. *Proc. Natl. Acad. Sci. USA* **100**, 9482-9487.

Sadatmansoori, S., MacDougall, J., Khademi, S., Cooke, L. S., Guarino, L., Meyer, E. F. and Forough, R. (2001). Construction, expression, and characterization of a baculovirally expressed catalytic domain of human matrix metalloproteinase-9. *Protein Expr. Purif.* **23**, 447-452.

Samochowiec, A., Grzywacz, A., Kaczmarek, L., Bienkowski, P., Samochowiec, J., Mierzejewski, P., Preuss, U. W., Grochans, E. and Ciechanowicz, A. (2010). Functional polymorphism of matrix metalloproteinase-9 (MMP-9) gene in alcohol dependence: family and case control study. *Brain Res.* **1327**, 103-106.

Shi, Y. and Ethell, I. M. (2006). Integrins control dendritic spine plasticity in hippocampal neurons through NMDA receptor and Ca2+/calmodulin-dependent protein kinase II-mediated actin reorganization. *J. Neurosci.* **26**, 1813-1822.

Stefanidakis, M., Bjorklund, M., Ihanus, E., Gahmberg, C. G. and Koivunen, E. (2003). Identification of a negatively charged peptide motif within the catalytic domain of progelatinases that mediates binding to leukocyte beta 2 integrins. *J. Biol. Chem.* **278**, 34674-34684.

Sternlicht, M. D. and Werb, Z. (2001). How matrix metalloproteinases regulate cell behavior. *Annu. Rev. Cell Dev. Biol.* **17**, 463-516.

Stoppini, L., Buchs, P. A. and Muller, D. (1991). A simple method for organotypic cultures of nervous tissue. *J. Neurosci. Methods* **37**, 173-182.

Szklarczyk, A., Lapinska, J., Rylski, M., McKay, R. D. and Kaczmarek, L. (2002). Matrix metalloproteinase-9 undergoes expression and activation during dendritic remodeling in adult hippocampus. *J. Neurosci.* **22**, 920-930.

Takacs, E., Nyilas, R., Szepesi, Z., Baracskay, P., Karlsen, B., Rosvold, T., Bjorkum, A. A., Czurko, A., Kovacs, Z., Kekesi, A. K. et al. (2010). Matrix metalloproteinase-9 activity increased by two different types of epileptic seizures that do not induce neuronal death: a possible role in homeostatic synaptic plasticity. *Neurochem. Int.* **56**, 799-809.

Tian, L., Stefanidakis, M., Ning, L., Van Lint, P., Nyman-Huttunen, H., Libert, C., Itohara, S., Mishina, M., Rauvala, H. and Gahmberg, C. G. (2007). Activation of NMDA receptors promotes dendritic spine development through MMP-mediated ICAM-5 cleavage. *J. Cell Biol.* **178**, 687-700.

Van den Steen, P. E., Proost, P., Wuyts, A., Van Damme, J. and Opdenakker, G. (2000). Neutrophil gelatinase B potentiates interleukin-8 tenfold by aminoterminal processing, whereas it degrades CTAP-III, PF-4, and GRO-alpha and leaves RANTES and MCP-2 intact. *Blood* **96**, 2673-2681.

Van den Steen, P. E., Van Aelst, I., Hvidberg, V., Piccard, H., Fiten, P., Jacobsen, C., Moestrup, S. K., Fry, S., Royle, L., Wormald, M. R. et al. (2006). The hemopexin and O-glycosylated domains tune gelatinase B/MMP-9 bioavailability via inhibition and binding to cargo receptors. *J. Biol. Chem.* **281**, 18626-18637.

Verpelli, C., Piccoli, G., Zanchi, A., Gardoni, F., Huang, K., Brambilla, D., Di Luca, M., Battaglioli, E. and Sala, C. (2010). Synaptic activity controls dendritic spine morphology by modulating eEF2-dependent BDNF synthesis. *J. Neurosci.* **30**, 5830-5842.

Wall, M. J., Robert, A., Howe, J. R. and Usowicz, M. M. (2002). The speeding of EPSC kinetics during maturation of a central synapse. *Eur. J. Neurosci.* **15**, 785-797.

Wang, X. B., Bozdagi, O., Nikitczuk, J. S., Zhai, Z. W., Zhou, Q. and Huntley, G. W. (2008). Extracellular proteolysis by matrix metalloproteinase-9 drives dendritic spine enlargement and long-term potentiation coordinately. *Proc. Natl. Acad. Sci. USA* **105**, 19520-19525.

Wilczynski, G. M., Konopacki, F. A., Wilczek, E., Lasiecka, Z., Gorlewicz, A., Michaluk, P., Wawrzyniak, M., Malinowska, M., Okulski, P., Kolodziej, L. R. et al. (2008). Important role of matrix metalloproteinase 9 in epileptogenesis. *J. Cell Biol.* **180**, 1021-1035.

Xu, J., Rodriguez, D., Petitclerc, E., Kim, J. J., Hangai, M., Moon, Y. S., Davis, G. E. and Brooks, P. C. (2001). Proteolytic exposure of a cryptic site within collagen type IV is required for angiogenesis and tumor growth *in vivo*. *J. Cell Biol.* **154**, 1069-1079.

Xu, T., Yu, X., Perlik, A. J., Tobin, W. F., Zweig, J. A., Tennant, K., Jones, T. and Zuo, Y. (2009). Rapid formation and selective stabilization of synapses for enduring motor memories. *Nature* **462**, 915-919.

Yamada, K. (2008). Endogenous modulators for drug dependence. *Biol. Pharm. Bull.* **31**, 1635-1638.

Yang, Y., Wang, X. B., Frerking, M. and Zhou, Q. (2008). Spine expansion and stabilization associated with long-term potentiation. *J. Neurosci.* **28**, 5740-5751.

Yao, J. S., Chen, Y., Zhai, W., Xu, K., Young, W. L. and Yang, G. Y. (2004). Minocycline exerts multiple inhibitory effects on vascular endothelial growth factor-induced smooth muscle cell migration: the role of ERK1/2, PI3K, and matrix metalloproteinases. *Circ. Res.* **95**, 364-371.

Yong, V. W. (2005). Metalloproteinases: mediators of pathology and regeneration in the CNS. *Nat. Rev. Neurosci.* **6**, 931-944.

Zhou, Q., Homma, K. J. and Poo, M. M. (2004). Shrinkage of dendritic spines associated with long-term depression of hippocampal synapses. *Neuron* **44**, 749-757.